

THE EFFECT OF SOIL TEXTURE IN SOIL MOISTURE RETRIEVAL FOR SPECULAR SCATTERING AT C-BAND

R. Prakash, D. Singh, and N. P. Pathak

Department of Electronics & Computer Engineering
Indian Institute of Technology Roorkee
Roorkee 247667, India

Abstract—The objective of this paper is to analyze the behavior of specular scattering for different soil texture fields at various soil moisture (m_v) and analyze the data to retrieve the soil moisture with minimizing the effect of the soil texture. To study the soil texture effect on specular scattering 10 different soil fields were prepared on the basis of change in soil constituents (i.e., percentage of sand, silt and clay) and experiments were performed in both like polarizations (i.e., HH -polarization and VV -polarization) at various incidence angles (i.e., varying incidence angle from 25° to 70° in step of 5°). Angular response of specular scattering coefficients (σ_{hh}° in HH -polarization and σ_{vv}° in VV -polarization) were analyzed for different soil texture fields with varying soil moisture content whereas the surface roughness condition for all the observations were kept constant. The changes in specular scattering coefficient values were observed with the change in soil texture fields with moisture for both like polarizations. Further, copolarization ratio ($P = \sigma_{hh}^\circ/\sigma_{vv}^\circ$) study was performed and it was observed that the dependency of copolarization ratio for change in soil texture field at constant soil moisture is less prominent whereas the value of copolarization ratio is varying with variation of moisture content. This emphasizes that copolarization ratio may be minimizing the effect of soil texture while observing the soil moisture on specular direction. Regression analysis is carried out to select the best suitable incidence angle for observing the moisture and texture at C-band in specular direction and 60° incidence angle was found the best suitable incidence angle. An empirical relationship between P and m_v was developed for the retrieval of m_v and the obtained relationship gives a good agreement with observed m_v . In addition, m_v was also retrieved

Received 4 May 2010, Accepted 25 June 2010, Scheduled 16 September 2010

Corresponding author: D. Singh (dharmfec@gmail.com).

through the Kirchhoff Approximation (SA) and a comparison was made with the retrieved results of empirical relationship. The empirical relationship outperformed the SA.

1. INTRODUCTION

Knowledge of spatial distribution of soil moisture is required in a number of applications such as hydrology, agriculture, weather monitoring etc. Soil moisture acts as an interface between the land surface and atmosphere and plays an important role in partitioning of precipitation into runoff and ground water storage [1, 2]. Scattering from soil in microwave domain is basically dependent on soil parameters, i.e., soil moisture, soil texture and surface roughness. Soil moisture is represented as the volumetric water content and defined as the fraction of the total volume of soil that is occupied by the water contained in the soil. Further, soil texture is a term commonly used to designate the proportionate distribution of the different sizes of particles in a soil. According to United States Department of Agriculture (USDA) system of nomenclature these soil particles are categorized as sand, silt and clay. Details on soil particle distribution are provided in Table 1 [3].

Most of the work for soil parameter characterization has been established for monostatic system [1, 2, 4–8] and lesser studies have been performed for bistatic system [9–16]. Bistatic configuration in contrast to monostatic configuration uses separate transmitter and receiver which are located individually. At present, several models have been proposed by the researchers in system conceptualization for having bistatic data from air-born/space-born mission [17–19]. In future, it is planned to send TanDem-X by German Aerospace Centre (DLR) in association with Astrium GmbH which will be the second satellite in series of TerraSAR-X and will provide the bistatic data in X-band [20].

Researches have shown that the soil dielectric constant is dependent on soil texture, along with it has been proved that change in dielectric constant with moisture shows its dependency on soil

Table 1. Nomenclature of soil constituent.

Name of soil separates	Diameter limits (mm)
Sand	2–0.05
Silt	0.05–0.002
Clay	Less than 0.002

texture [21–24]. Microwave scattering is highly dielectric dependent parameter which shows the feasibility of studying the soil texture from remotely sensed data in microwave domain [8, 11, 12, 22, 23]. Some studies have been carried out to analyze the soil texture effect on scattering coefficient but the individual soil constituent response on specular scattering is under research.

Most of the research work in bistatic configuration to characterize the soil parameters is simulation work and less experimental studies have been performed. Wu et al. [16] made a simulation study for bistatic scattering by varying the surface roughness and made a comparison for Advance Integral Equation Model (AIEM) with the Small Perturbation Model (SPM), Kirchhoff Scalar Approximation (SA) and Kirchhoff Stationary Phase Approximation (SPA) for their respective validity range. Pierdicca et al. [15] has attempted to retrieve the soil moisture by performing a simulation study based on AIEM model but does not consider the soil texture effect in their study. Nashashibi and Ulaby [13] explore the nature of bistatic scattering from soil surface by performing the measurement at 35 GHz. They have also shown that the calculation based on Kirchhoff scalar Approximation provides good agreement between the theory and observation. Even though, this paper does not mention the effect of soil texture on scattering and explains the scattering behavior based on the moisture and surface roughness only. Ceraldi et al. [11] provided a scheme for the retrieval of soil moisture in bistatic case minimizing the effect of surface roughness but did not consider the effect of soil texture. De Roo and Ulaby [12] conducted the experiment to determine the nature of the bistatic scattering from rough dielectric surface at 10 GHz. The observation was obtained for specular scattering and it was shown that the Kirchhoff Scalar Approximation provide good agreement with the observed data. Studies carried out in the field of bistatic reveal that for soil surface characterization the observation should be made in specular direction [11–15]. In this paper, we have prepared different field for known soil texture constituent that is by varying the soil constituent (i.e., percentage of sand, silt and clay) and prepared 10 fields that represent lower sand value to higher sand value and similarly for silt and clay. The main aim of this paper is to know the individual effect of soil constituent on specular scattering in one hand and in other hand to know the effect of specular scattering after changing the moisture level in these fields. Further, an algorithm has been proposed for the retrieval of soil moisture which can minimize the effect of soil texture.

This paper is organized as follows. In Section 2, there is a brief description of experiment performed with the specification of soil texture fields and soil moisture measurements. Further, modeling

approach for soil moisture retrieval is illustrated. Section 3 treat the results and discussion part which include study of specular scattering coefficient with change in soil texture fields and soil moisture, along with the development of empirical relationship between soil moisture and copolarization ratio. Finally, in Section 4 conclusions have been drawn.

2. METHODOLOGY

2.1. Field Preparation and Field Data Analysis

Ten different soil texture fields were analyzed for their response to specular scattering coefficient. Different soil texture fields were artificially prepared by changing the percentage of soil constituent, i.e., sand, silt, and clay. Sieve analysis and hydrometric tests were conducted to find out the percentage of sand, silt, and clay in soil. Variations in sand percentage, silt percentage, and clay percentage were from 85.3% to 2.3%, 70.6% to 7.5%, and 81.6% to 2.5% respectively and details of soil constituents for these fields are given in Table 2. Sieve analysis using various sieves of different mesh opening (4.75 mm to 0.075 mm) were used to calculate the percentage of sand. The percentage of soil retained on each sieve is calculated on the basis of the total mass of the soil sample. In addition, soil fraction finer than 0.075 mm were separated out for further hydrometric test. Hydrometric test was carried out for particle size lesser than 0.075 mm to determine the percentage of silt and clay in soil [25]. To check the

Table 2. Soil constituent of 10 different soil texture fields used for observations.

	% of Sand	% of Silt	% of Clay	% of Gravels
Field 1	85.3	7.5	2.5	4.1
Field 2	62.6	26.1	5.3	5.2
Field 3	47.2	32.7	15.4	4.5
Field 4	24.6	20.1	48.7	6.3
Field 5	25.5	41.3	21.7	11.2
Field 6	17.4	51.2	20.8	10.4
Field 7	11.2	70.6	4.8	13.1
Field 8	12.8	29.3	51.5	5.6
Field 9	7.5	23.4	64.2	4.8
Field 10	2.3	10.3	81.6	5.6

Table 3. Volumetric soil moisture values used for each field.

	m_{v1} $\text{cm}^3\text{cm}^{-3}$	m_{v2} $\text{cm}^3\text{cm}^{-3}$	m_{v3} $\text{cm}^3\text{cm}^{-3}$	m_{v4} $\text{cm}^3\text{cm}^{-3}$	m_{v5} $\text{cm}^3\text{cm}^{-3}$	m_{v6} $\text{cm}^3\text{cm}^{-3}$
Field 1	0.028	0.083	0.201	0.265	0.346	0.420
Field 2	0.030	0.096	0.183	0.281	0.379	0.403
Field 3	0.031	0.104	0.174	0.240	0.351	0.441
Field 4	0.023	0.108	0.197	0.255	0.395	0.415
Field 5	0.028	0.114	0.181	0.270	0.380	0.411
Field 6	0.024	0.091	0.207	0.258	0.373	0.426
Field 7	0.025	0.097	0.168	0.261	0.361	0.408
Field 8	0.027	0.084	0.212	0.274	0.382	0.434
Field 9	0.023	0.081	0.176	0.176	0.386	0.441
Field 10	0.026	0.098	0.185	0.255	0.390	0.455
mean	0.027	0.096	0.188	0.261	0.374	0.425
STDEV	0.003	0.011	0.015	0.012	0.017	0.017

specular scattering response for soil moisture variation observations were made on dry soil (average volumetric soil moisture content is $0.027 \text{ cm}^3\text{cm}^{-3}$) as well as on moist soil, which were artificially irrigated. Moisture variations were made from nearly dry soil to high moisture content ($m_v = 0.425 \text{ cm}^3\text{cm}^{-3}$) and details are provided in Table 3. For moisture measurements, 10 soil samples of up to 5 cm depth were chosen randomly and average value of soil moisture were reported. Firstly these moist samples were weighted, afterward kept for 24 hours at 110°C for drying and subsequently these dry samples were weighted. Volumetric soil moisture (m_v) was measured with the help of (1) [5].

$$m_v = \frac{w_{moist} - w_{dry}}{w_{dry}} \times \rho_b \quad (1)$$

where w_{moist} and w_{dry} are weight of moist and dry soil sample, respectively and ρ_b is the soil bulk density. Further, root mean square surface height and correlation length of each field was measured with pin profile meter. Surface roughness values for all observations were kept constant and average value of rms height and correlation length was reported. Average value and standard deviation for rms surface height was 0.36 cm and 0.04 cm, respectively and for correlation length was 5.57 cm and 0.95 cm respectively.

Table 4. System parameters.

Antenna type	Dual polarized pyramidal horn
Central frequency	6 GHz
Frequency band width	2 GHz
Beam width in H -plane	16.7°
Beam width in E -plane	15.2°
Antenna gain	21 dB
Cross-polarization isolation	40 dB
Platform height	3 m

2.2. Experimental Setup

In order to retrieve the specular scattering coefficient for different soil texture fields with varying soil moisture conditions a C-band bistatic scatterometer setup was indigenously developed. C-band pyramidal horn antenna was mounted on a movable platform of 3 meter height and its parameters are listed in Table 4. Developed scatterometer setup is capable of taking observation in both like polarizations, i.e., HH -polarization and VV -polarization and incidence angle varying from 25° to 70° in step of 5°. Field size of different soil fields was 2 m × 2 m. The details regarding the selection of the field size and the position of horn antenna is provided in Appendix A. Further, the formulation used to calculate the specular scattering coefficient can be found from the reference Prakash et al. [14].

2.3. Theoretical Approach

The Kirchhoff Scalar Approximation provides the reasonable good fit to the experimental data in specular direction [12–15]. The formulation has been used to retrieve the soil moisture with a priori information of rms surface height and correlation length and the results were compared with the proposed empirical approach. Final expression of specular scattering coefficient for the Kirchhoff Scalar Approximation is given in (2) and detailed expressions are provided in Appendix B

$$\sigma_{pqc} = \pi k^2 |a_o|^2 \delta(0) \delta(0) e^{-q_z^2 s^2} + (|a_o| kl/2)^2 \exp\left(- (2k \cos \theta)^2 s^2\right) \sum_n \left(\frac{\left((2k \cos \theta)^2 s^2 \right)^n}{n!n} \right) \quad (2)$$

2.4. Modeling Approach

Figure 1 illustrates the flow chart of the modeling approach to carry out the soil moisture retrieval by minimizing the soil texture effect. Following points discuss in detail the approach that has been followed in the development of the proposed algorithm.

1. Angle of incidence is important dependent parameter for deciding the sensor parameter and retrieval algorithm. Therefore it is important to know the angular behavior of the specular scattering coefficient for different soil texture and moisture conditions. It is difficult to segregate the individual effect like incidence angle effect on texture and moisture therefore there is a need to carry

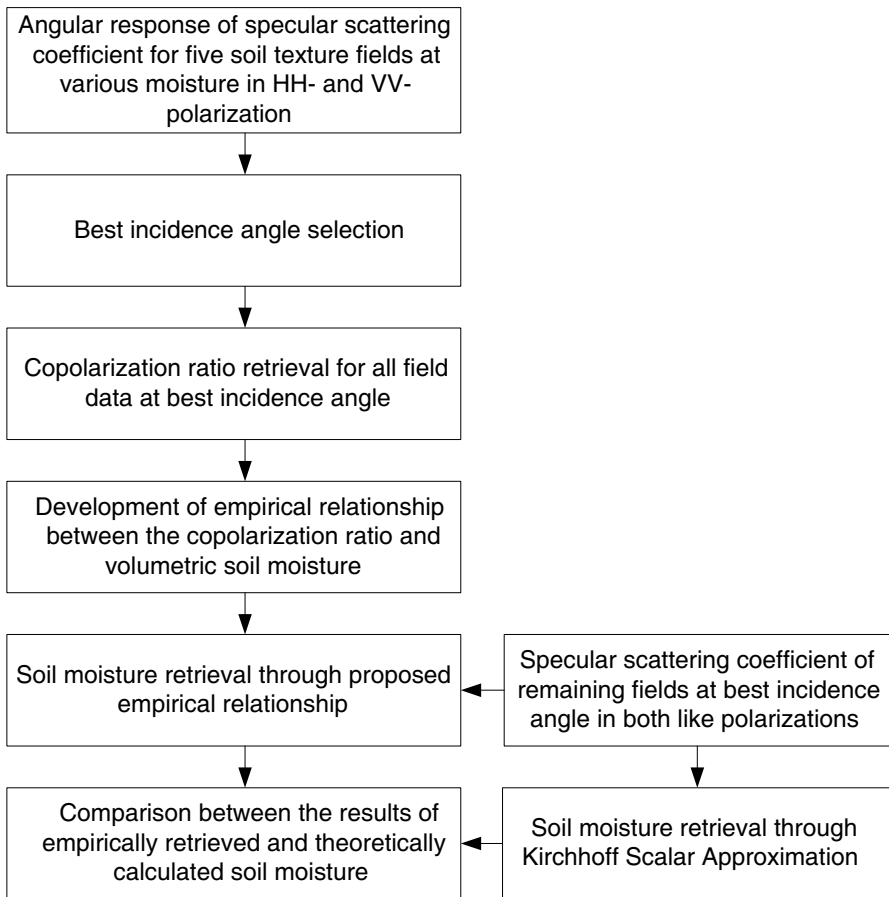


Figure 1. Flow chart for the proposed algorithm.

out some statistical analysis by which the effect of the surface parameters on specular scattering coefficient on different incidence angle may be observed. One of the methods is regression analysis with coefficient of determination (R^2) tell about the relationship between dependent and independent variables on the one hand and on the other hand the extent to which dependent variable (for this case specular scattering coefficient) depend on the independent variable (for our case soil texture and soil moisture). Therefore, multiple regression analysis was performed to realize the incidence angle at which the specular scattering coefficient best represent the different soil parameters.

2. The effect of soil texture on specular scattering coefficient prompt to minimize its effect for soil moisture retrieval. Therefore, it is important to carry out the copolarization ratio ($\sigma_{hh}^\circ/\sigma_{vv}^\circ$) study and check how it may be helpful to minimize the soil texture effect on the specular scattering. A detailed analysis of copolarization ratio was performed for various soil texture fields with different moisture content. The obtained results are quite encouraging and imply that soil texture has negligible effect on copolarization ratio and the change in the copolarization ratio is obtained only with the soil moisture.
3. The best incidence angle selection (step 1) and the minimization of the soil texture effect on copolarization ratio as well as its dependence on soil moisture content only (step 2), suggest a relationship between the copolarization ratio and volumetric soil moisture content. An empirical relationship has been developed between the copolarization ratio and soil moisture with good coefficient of determination. The soil moisture content of any field can be determined by the inversion of this empirical relationship.

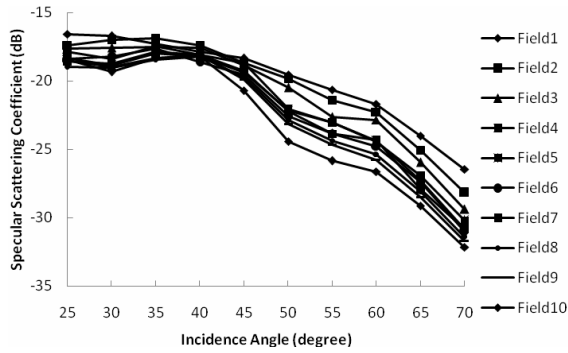
3. RESULTS AND DISCUSSION

3.1. Response of Specular Scattering Coefficient for Soil Texture

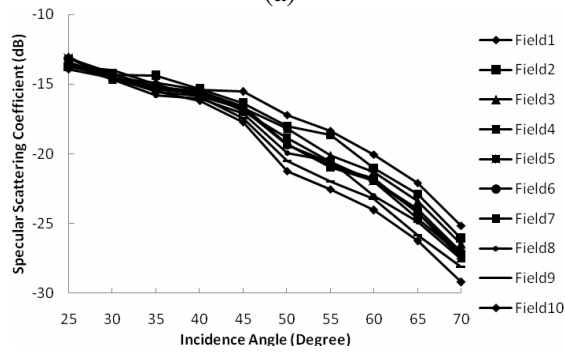
Angular variation of specular scattering coefficient for different soil texture and moisture for both like polarizations are shown in Figures 2 and 3 and details about the fields are given in Tables 2 and 3.

3.1.1. Specular Scattering Response for Soil Texture in HH-polarization for Dry Soil

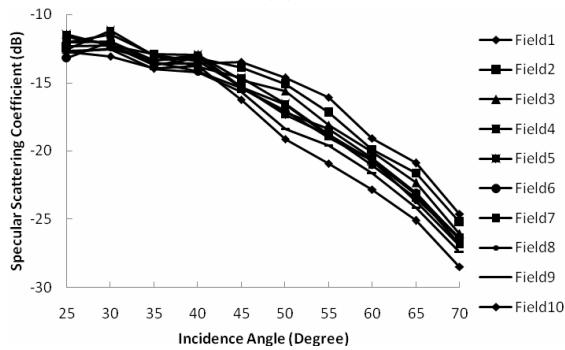
Discrimination in specular scattering coefficient can be observed in different soil texture fields at C-band for dry soil (Figure 2(a)). Field 1 (sand = 85.3%, silt = 7.5%, and clay = 2.5%) which consists of



(a)



(b)



(c)

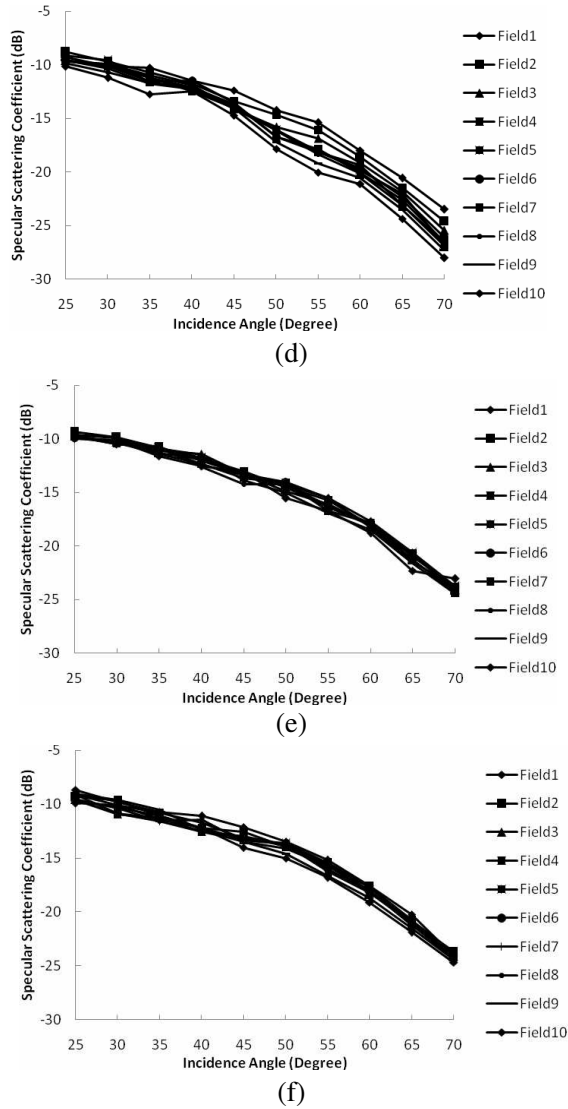


Figure 2. Specular scattering coefficient behavior with incidence angle for 10 different soil texture fields in *HH*-polarization. (a), (b), (c), (d), (e), and (f) show volumetric soil moisture content $0.027 \text{ cm}^3 \text{ cm}^{-3}$, $0.096 \text{ cm}^3 \text{ cm}^{-3}$, $0.188 \text{ cm}^3 \text{ cm}^{-3}$, $0.261 \text{ cm}^3 \text{ cm}^{-3}$, $0.374 \text{ cm}^3 \text{ cm}^{-3}$, and $0.425 \text{ cm}^3 \text{ cm}^{-3}$ respectively.

maximum amount of sand have dynamic range in specular scattering coefficient of 9.8 dB while Field 10 (sand = 2.3%, silt = 10.3%, and clay = 81.6%) which contains the maximum amount of clay have dynamic range of 13.6 dB with incidence angle. The observation suggests that the discrimination between sandy soil and clay soil can be made on the basis of the specular scattering coefficient. It was observed that with the decrease of sand percentage in soil (Field 1 to Field 4) the dynamic range of specular scattering coefficient increases, whereas the increase in scattering coefficient occurs with the increase in clay percentage in soil (Field 7 to Field 10). Further, major changes in silt percentage (Field 5 to Field 7) have lesser effect on specular scattering coefficient and the dynamic ranges remain approximately 12.2 dB. These observations are clearly evident in Figure 2(a). Therefore it may be inferred that when the silt constituent in the soil is changed from the 41.3% to 70.6% it has the minimum effect on the specular scattering coefficient at C-band and HH -polarization. Further, in case of higher incidence angle ($\geq 45^\circ$) decrease in specular scattering coefficient is observed with the decrease in sand percentage, i.e., decreasing the sand percentage from 85.3% to 24.6%, whereas keeping the percentage of sand and clay lower in soil and making the changes in silt percentage in major amount does not affect the specular scattering coefficient significantly and provides a kind of saturation in specular scattering coefficient (Figure 2(a)). Additionally, a decrease in specular scattering coefficient is again observed with the increase in clay percentage from 51.5% to 81.6% (Figure 2(a)).

The observation made with different soil texture field for dry soil at C-band in HH -polarization suggest that the higher incidence angle ($\geq 45^\circ$) better discriminate between different soil texture field and the changes made in sand constituent and clay constituent have greater effect on the specular scattering coefficient, where as the change in silt constituent has very less effect on specular scattering coefficient.

3.1.2. Specular Scattering Response for Soil Texture in HH -polarization for Moist Soil

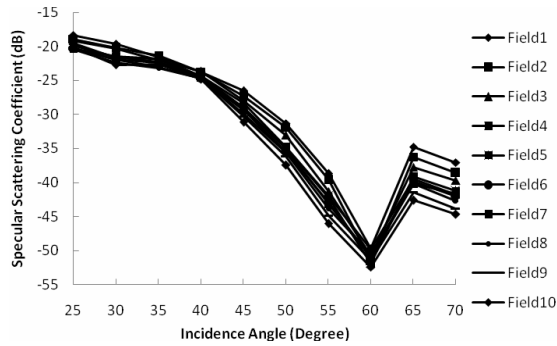
To study the effect of soil moisture on different soil texture fields, fields were irrigated artificially. The details about the fields are given in Table 3. Figures 2(b), 2(c), 2(d), 2(e), and 2(f) explain the angular behavior of specular scattering coefficient when the volumetric soil moisture contents were $0.096 \text{ cm}^3\text{cm}^{-3}$, $0.188 \text{ cm}^3\text{cm}^{-3}$, $0.261 \text{ cm}^3\text{cm}^{-3}$, $0.374 \text{ cm}^3\text{cm}^{-3}$ and $0.425 \text{ cm}^3\text{cm}^{-3}$, respectively for 10 different soil texture fields. The effect of soil texture on specular scattering can be noticed for lower soil moisture contents, i.e., with the change in soil texture field, significant changes in specular scattering

coefficient can be observed (Figures 2(b), 2(c), and 2(d)). The dynamic range of 11.2 dB, 12.3 dB, and 13.4 dB was observed at volumetric soil moisture contents $0.096 \text{ cm}^3 \text{ cm}^{-3}$ for Field 1, Field 2 and Field 3, respectively. The dynamic range for Field 4 to Field 8 is approximately 14 dB and in case of Field 9 and Field 10 the dynamic range is 14.5 dB and 15.7 dB respectively (Figure 2(b)). These observations clearly signify the soil texture effect on specular scattering coefficient in the presence of lower soil moisture (i.e., $0.096 \text{ cm}^3 \text{ cm}^{-3}$) and infer that the Field 1 to Field 2 and Field 9 and Field 10 which has the higher amount of the sand and clay respectively has key changes in specular scattering coefficient while Field 4 to Field 8 which has higher amount of the silt has almost same response for the specular scattering coefficient. Further, with the increase in soil moisture content, it was observed that at volumetric soil moisture content $0.188 \text{ cm}^3 \text{ cm}^{-3}$ and $0.261 \text{ cm}^3 \text{ cm}^{-3}$, the dynamic range for Field 3 to Field 8 were approximately same whereas Field 1 and Field 2 that possess the high amount of sand (85.3% and 62.6% respectively) have lowest dynamic range while Field 9 and Field 10 that possess the high amount of clay content (64.2% and 81.6% respectively) have maximum dynamic range (Figures 2(c) and 2(d)). The effect of soil texture on specular scattering coefficient is difficult to observe at high moisture content ($m_v = 0.374 \text{ cm}^3 \text{ cm}^{-3}$ and $0.425 \text{ cm}^3 \text{ cm}^{-3}$), i.e., with the change in soil texture very less changes occur in specular scattering coefficient (Figures 2(e) and 2(f)). The effect may arise due to high dielectric constant of water, i.e., after some particular soil moisture content saturation occurs and moisture effect dominates the soil texture effect. Further, Figures 2(b) to 2(d) suggest that for soil moisture less than or equal to $0.261 \text{ cm}^3 \text{ cm}^{-3}$, higher incidence angle ($\geq 45^\circ$) provide the better changes in specular scattering coefficient for the change in sand constituent (Field 1 to Field 3) and clay constituent (Field 8 to Field 10) but lesser changes can be observed for the change in silt constituent (Field 4 to Field 7).

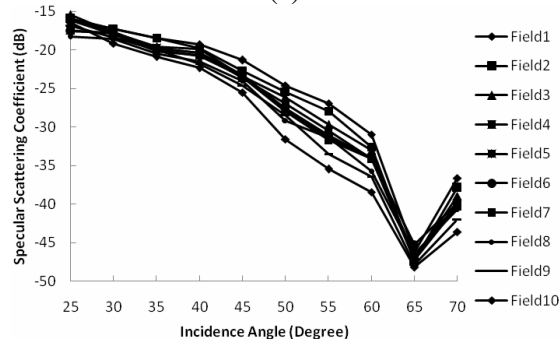
Observation with the moisture content in soil for different soil texture field at C-band in *HH*-polarization infer that the sand and clay constituent of the soil has its effect on specular scattering coefficient for soil moisture content up to $0.261 \text{ cm}^3 \text{ cm}^{-3}$ whereas the silt constituent has the minimum effect. The effect is more prominent at higher incidence angel ($\geq 45^\circ$). Soil moisture content higher than $0.261 \text{ cm}^3 \text{ cm}^{-3}$ provides the specular scattering coefficient with minimum changes was observed with the change in soil texture and only the angular variation was observed.

3.1.3. Specular Scattering Response for Soil Texture in VV-polarization for Dry Soil

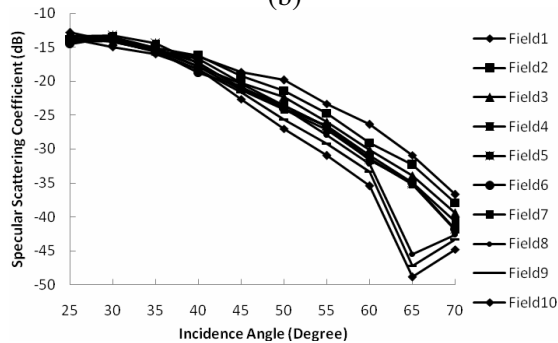
Figure 3(a) provides the insight for the variation in specular scattering coefficient with incidence angle in VV-polarization for 10 different soil texture fields for dry soil (i.e., volumetric soil moisture is $0.027\text{ cm}^3\text{ cm}^{-3}$). The change in specular scattering coefficient was



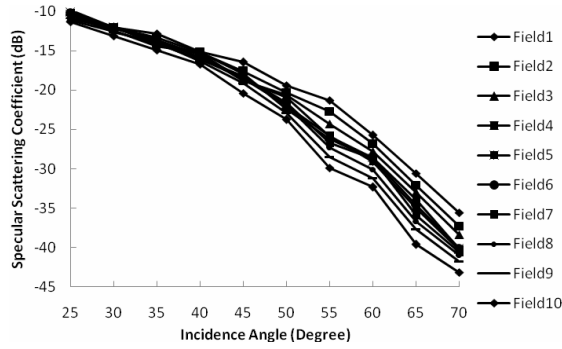
(a)



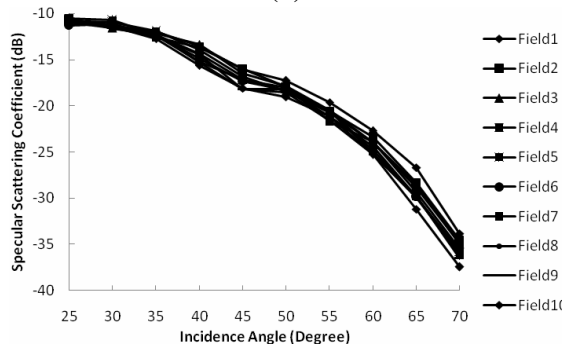
(b)



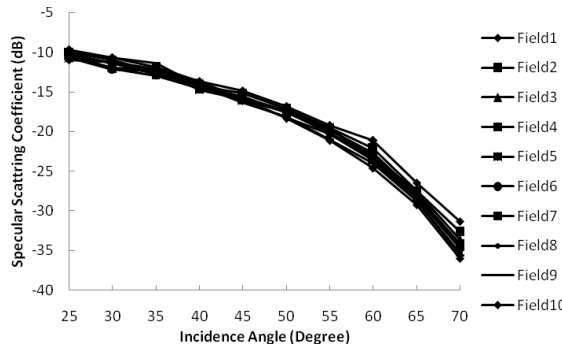
(c)



(d)



(e)



(f)

Figure 3. Specular scattering coefficient behavior with incidence angle for 10 different soil texture fields in *VV*-polarization. (a), (b), (c), (d), (e), and (f) show volumetric soil moisture content $0.027 \text{ cm}^3\text{cm}^{-3}$, $0.096 \text{ cm}^3\text{cm}^{-3}$, $0.188 \text{ cm}^3\text{cm}^{-3}$, $0.261 \text{ cm}^3\text{cm}^{-3}$, $0.374 \text{ cm}^3\text{cm}^{-3}$, and $0.425 \text{ cm}^3\text{cm}^{-3}$ respectively.

observed with the change in soil texture in VV -polarization also, as was the case with HH -polarization. Figure 3(a) explains the behavior of specular scattering coefficient for dry soil and the observation infers that higher incidence angle ($\geq 45^\circ$) has better discrimination for different soil texture field than at lower incidence angle. It can be observed from Figure 3(a) that at 60° incidence angle a sharp decrease in specular scattering coefficient occur for all the 10 different soil texture fields. This phenomenon may be due to Brewster angle effect in VV -polarization. Brewster angle is characterized as the incidence angle at which all the incident power is transmitted and theoretically there should be no reflected power. But, the undulation and inhomogeneity in the medium provide lower values of specular scattering coefficient.

The observation at C-band in VV -polarization for dry soil with different soil texture field suggests the utilization of the higher incidence angle.

3.1.4. Specular Scattering Response for Soil Texture in VV -polarization for Moist Soil

Figures 3(b)–(f) explain the angular behavior of specular scattering coefficient when the volumetric soil moisture contents were $0.096 \text{ cm}^3 \text{ cm}^{-3}$, $0.188 \text{ cm}^3 \text{ cm}^{-3}$, $0.261 \text{ cm}^3 \text{ cm}^{-3}$, $0.374 \text{ cm}^3 \text{ cm}^{-3}$ and $0.425 \text{ cm}^3 \text{ cm}^{-3}$, respectively for 10 different soil texture fields in VV -polarization. A shift in Brewster angle from 60° to 65° is observed with the increase in soil moisture, i.e., $m_v = 0.096 \text{ cm}^3 \text{ cm}^{-3}$ (Figure 3(b)). This occurs due to the change in dielectric constant of soil with the moisture that causes the shift in Brewster angle. Further, at volumetric soil moisture content $0.188 \text{ cm}^3 \text{ cm}^{-3}$ only the soil with higher clay content (Field 8, Field 9, and Field 10) exhibit the Brewster angle effect while the soil with higher sand or silt content (Field 1 to Field 7) did not exhibit Brewster angle (Figure 3(c)). This may be due to the lower dielectric constant of soil having greater amount of clay constituent and high dielectric constant of soil having high amount of sand or silt constituent. Similar results were also found by De Roo and Ulaby [12] and Nashashibi and Ulaby [13]. At high moisture values the Brewster angle effect is not observed (Figures 3(d), 3(e), and 3(f)). Further, it may be noticed from Figures 3(e) and 3(f) that when the moisture content in soil is high ($m_v = 0.374 \text{ cm}^3 \text{ cm}^{-3}$ and $0.425 \text{ cm}^3 \text{ cm}^{-3}$ respectively), approximately same specular scattering coefficient values are obtained with the change in soil texture at all incidence angle. Albeit, at these high moisture contents the dynamic range for soil having high amount of sand (Field 1) and high amount of clay (Field 10) show significant changes. Dynamic range for Field 1 (sand = 85.3%, silt = 7.5%, and

clay = 2.5%) is 22.9 dB and dynamic range for Field 10 (sand = 2.3%, silt = 10.3%, and clay = 81.6%) is 26.6 dB.

The observation made with moist soil for different soil texture field at C-band in VV -polarization suggest the use of higher incidence angle ($\geq 45^\circ$) as was the case with HH -polarization. The Brewster angle effect was not observed for soil moisture content equal to or greater than $0.261 \text{ cm}^3 \text{ cm}^{-3}$ and the and the discrimination for the high amount of sand in soil (Field 1) and high amount of clay in soil (Field 10) can be made at all soil moisture values. Further, the effect of silt constituent on specular scattering coefficient is minimum as was observed in HH -polarization.

3.2. Copolarization Ratio Response for Soil Texture with Different Soil Moisture Contents

Figures 4 and 5 represent the change in specular scattering coefficient with different soil texture at various soil moistures in HH - and VV -polarization respectively at 60° incidence angle which is obtained through the regression analysis and detail regarding the regression is discussed in Section 3.3. The change in specular scattering coefficient for different field is clearly evident for the both like polarizations. This signifies the effect of soil texture on the specular scattering coefficient. The copolarization ratio study was carried out to check the effect of soil texture on copolarization ratio. Figure 6 explains the behavior of the copolarization ratio for the change in soil texture field. It is evident from the figure that the value of copolarization ratio is approximately constant with variation of soil texture at constant soil moisture which

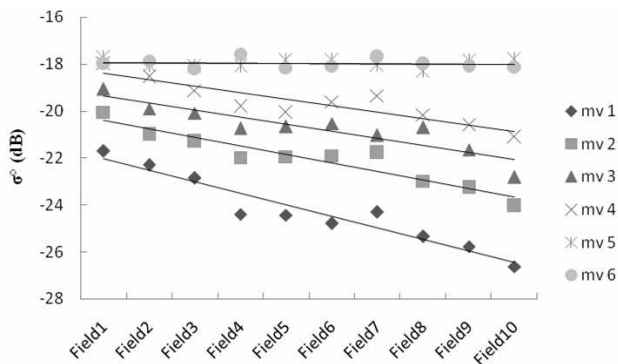


Figure 4. Specular scattering coefficient variation with change in soil texture field at different moisture condition for HH -polarization.

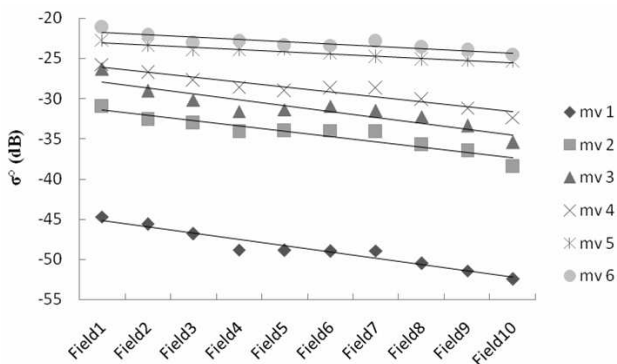


Figure 5. Specular scattering coefficient variation with change in soil texture field at different moisture condition for *VV*-polarization.

indicates that copolarization ratio is less sensitive for soil texture. The change in copolarization ratio is observed with the change in soil moisture content. The higher value of copolarization ratio is found for the lowest value of soil moisture content and vice versa.

The study with the copolarization ratio suggest that it is almost independent to the changes made in soil constituent, i.e., the variation of sand percentage, silt percentage or clay percentage at constant moisture. Therefore, it may be inferred that the copolarization ratio minimizes the soil texture effect and the variation in copolarization ratio can be observed with the variation in soil moisture content only.

3.3. Soil Moisture Retrieval

Step 1: The discussion made in Section 3.1 and from Figures 2 and 3 it is observed that specular scattering coefficient is highly dependent on angular variation for all soil texture fields in both like polarizations. Now in accordance to Step 1 of modeling approach (Section 2.4), multiple regression analysis was carried out keeping the soil texture (i.e., percentage of sand, silt, and clay) and soil moisture as independent variable and specular scattering coefficient as dependent variable. Results of regression analysis are shown in Table 5. Incidence angle greater than 45° provides the R^2 values that are always greater than 0.85 and 0.80 and SE is less than 1.01 and 1.50 in *HH*- and *VV*-polarization respectively, which infer that higher incidence angle better correlate the specular scattering coefficient with soil texture and soil moisture as we observed experimentally also. The lower value of R^2 and higher value of SE for *VV*-polarization in comparison to *HH*-

Table 5. Multiple regression analysis results.

<i>HH</i> -Pol			<i>VV</i> -Pol		
Incidence angle (degree)	R^2	SE	Incidence angle (degree)	R^2	SE
25	0.80	1.46	25	0.75	1.43
30	0.78	1.48	30	0.76	1.50
35	0.76	1.00	35	0.70	1.55
40	0.80	1.07	40	0.80	1.74
45	0.86	0.90	45	0.80	1.48
50	0.85	0.96	50	0.81	1.42
55	0.89	0.98	55	0.84	1.37
60	0.92	0.78	60	0.89	1.05
65	0.86	0.91	65	0.80	1.44
70	0.85	1.01	70	0.83	1.49

polarization at higher incidence angle may be due to the Brewster angle effect observed in *VV*-polarization. The observation at lower incidence angle provides low R^2 and high SE, which led to conclude that lower incidence angle are not suitable for characterizing the soil parameters when observations are made in specular direction at C-band. Use of higher incidence angle for soil parameter characterization has also been recommended by Singh and Dubey [10], Cereldi et al. [11], Nashashibi and Ulaby [13], Prakash et al. [14] for scattering in specular direction. The maximum value of R^2 is obtained at 60° incidence angle for both like polarizations. Hence, we have considered 60° as the best suitable incidence angle for observing soil texture and soil moisture at C-band in specular direction.

Step 2: From Step 1 it is observed that 60° incidence angle describe the best incidence angle for soil parameter characterization when observation are made in specular direction. Our further discussion will be concentrated on specular scattering coefficient values obtained at this best incidence angle. The discussion made in Section 3.2 clearly signifies from the Figures 4 and 5 that specular scattering coefficient is a sensitive parameter for different soil texture field in both like polarizations. Though, at higher moisture we can observe the approximate same specular scattering coefficient values. The effect may be explained that at higher moisture value the proportion of water in soil increases drastically and the effect of soil texture is less

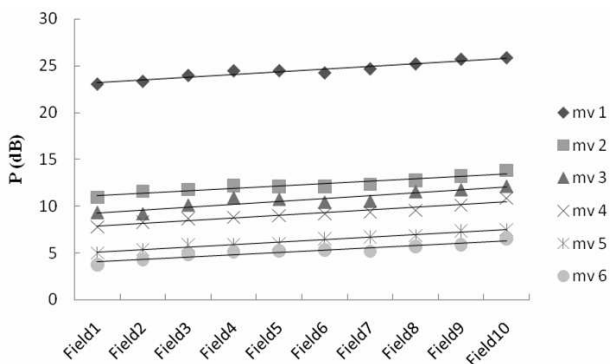


Figure 6. Copolarization ratio variation with change in soil texture field at different moisture condition.

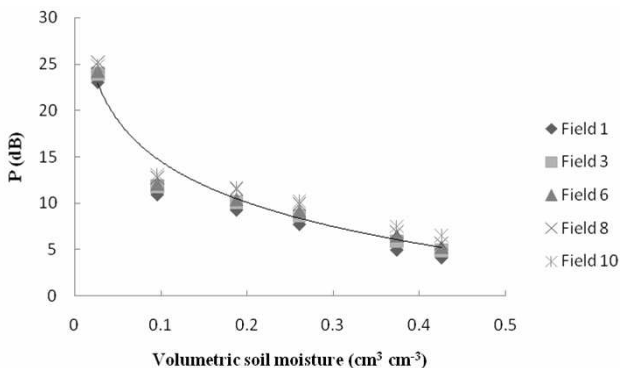


Figure 7. Change in copolarization ratio with volumetric soil moisture for different soil texture field.

prominent. This phenomenon is clearly visible in case of both like polarization for volumetric soil moisture approximately $0.374 \text{ cm}^3 \text{ cm}^{-3}$ and higher. Further, the discussions in Section 3.2 also suggest the minimization of soil texture effect with the copolarization ratio and the change in copolarization ratio with moisture content only (Figure 6).

Step 3: Copolarization ratio study suggest a relationship between the copolarization ratio (P) and soil moisture (m_v) that is almost independent to the effect of soil texture. Five different soil texture fields (Field 1, Field 3, Field 6, Field 8 and Field 10) with various soil moisture values were chosen for the development of the empirical relationship and the remaining five fields (Field 2, Field 4, Field 5, Field 7 and Field 9) were kept for the validation purposes. Figure 7

shows the graph that has been plotted between the copolarization ratio and volumetric soil moisture content for five different soil texture fields on the basis of which the empirical relationship has to be developed. The empirical relation has been developed between copolarization ratio (P) and volumetric soil moisture (m_v) based upon these five soil texture fields. The developed empirical relationship is given in (3) with R^2 values always greater than 0.95 and SE is less than 0.51.

$$P = a \times \ln(m_v) + b \quad (3)$$

The values of constant a and b are respectively -6.562 and -0.4658 . These values are average of all the fields with the standard deviation of 0.081 and 0.1477 respectively for a and b .

The developed empirical relationship is tested for retrieval of soil moisture content with the same set of fields and RMSE was 0.015 for retrieved soil moisture content. Furthermore, the remaining other five soil fields that were kept for validation of developed empirical relationship, the obtained results for the volumetric soil moisture provide the RMSE of 0.021. In addition, F-test has been carried out to check the validity of retrieved results through empirical relationship. F-test determines how unlikely the result have been if the two values compared really weren't different. The level of statistical significance is kept 0.05. The critical F value for our measurement is 1.86 and the F value for retrieved result of m_v in case of testing data is 1.33 and

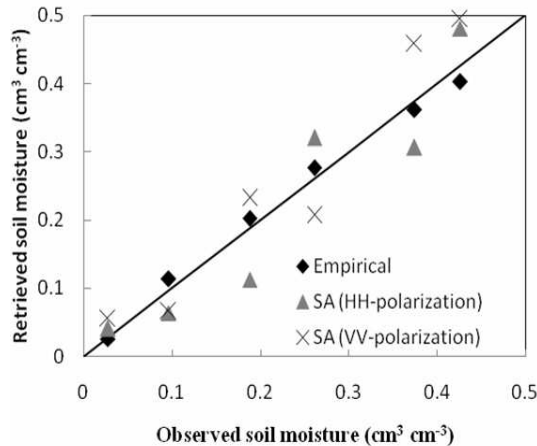


Figure 8. Comparison between observed value of soil moisture and soil moisture retrieved through developed empirical relationship, Kirchhoff Scalar Approximation in HH -polarization and Kirchhoff Scalar Approximation in VV -polarization.

for validation data is 1.23. The F values are smaller than the critical F value which approves the significance of the developed empirical relationship.

A comparison has been drawn between soil moisture values retrieved through empirical relationship and Kirchoff Scalar Approximation (SA). Figure 8 shows the comparison for observed values and the retrieved values of m_v through developed empirical relationship and SA in HH -polarization and VV -polarization. The RMSE are 0.021, 0.079 and 0.095 for empirical relationship, SA in HH -polarization and VV -polarization respectively. The results clearly show that empirical relationship performed better than the SA in both like polarizations. The phenomenon can be explained in the term of the limitation of SA in characterizing the different soil texture fields while the empirical relationship takes into account the effect of soil texture.

4. CONCLUSION

The present study explains the behavior of specular scattering coefficient for different soil texture fields and its variation with soil moisture at C-band in both like polarizations. The study reveals that the specular scattering coefficient changes with the change in soil texture, and the major changes were observed for the change in sand constituent and clay constituent where the silt constituent in the soil provided minimum effect on the specular scattering coefficient for both like polarizations in C-band. The effect of sand, silt and clay constituent was observed up to soil moisture content $0.261 \text{ cm}^3 \text{ cm}^{-3}$ whereas approximately the same specular scattering coefficient was observed for the change in soil constituent at soil moisture content $0.374 \text{ cm}^3 \text{ cm}^{-3}$ and $0.425 \text{ cm}^3 \text{ cm}^{-3}$. Angular variation of specular scattering coefficient for different soil texture infers that the higher incidence angles ($\geq 45^\circ$) are quite suitable for observing the soil texture effect. It is noticed that generally in the models soil texture effect is not considered for retrieving the soil moisture which may affect the accuracy of the retrieved soil moisture because texture is quite dependent on specular scattering coefficient. Therefore, to minimize the soil texture effect copolarization ratio study was performed. Copolarization ratio study revealed that the change in soil constituent had the least effect on the copolarization ratio, and approximately same copolarization ratio was observed for all soil texture fields at constant soil moisture. It was also observed that the change in copolarization ratio was obtained with the change in soil moisture content. It indicates that copolarization ratio may retrieve the soil moisture quite accurately because it is less sensitive to soil texture. Therefore, we have

developed an empirical relationship between copolarization ratio and volumetric soil moisture. The obtained retrieved results are in good agreement with ground data. The empirical relationship performed better than the Kirchoff Scalar Approximation. Results obtained are very promising, and study may be explored for soil moisture monitoring with bistatic air born/space born mission.

ACKNOWLEDGMENT

Authors are thankful to Department of Science and Technology, India and Department of Earth Sciences, India for providing the fund to support the work.

APPENDIX A.

Determination of point in x - y plane is the most important problem in the radar reflectivity measurement system. As in our system the angle of incidence of the wave has been changed at a step of 5° from

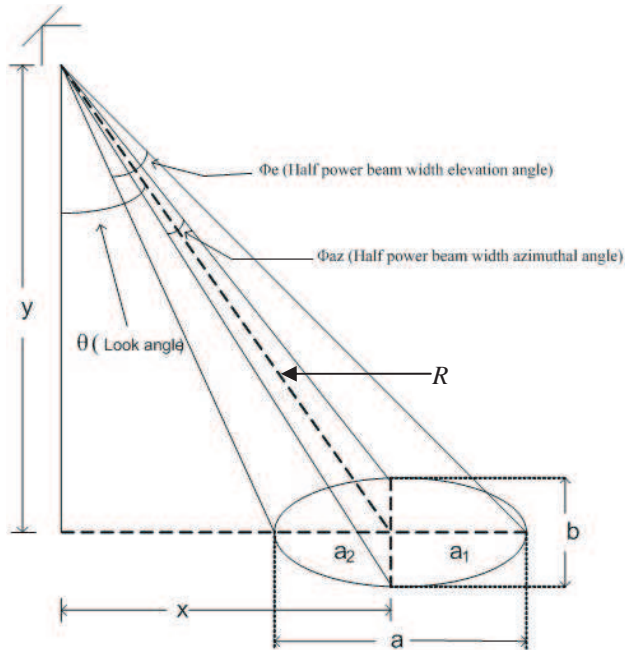


Figure A1. Geometry for the calculation of antenna position in x - y plane for fixed illumination area.

25° to 70°, therefore the position of the antennas has to be maintained such that the main lobe of the radiation pattern falls on the given field area. For finding out the values of x and y the illumination area is considered to be elliptical in shape. The geometry for the setup is provided in Figure A1. Equations (A1) and (A2) are used for the determination of the x and y positions of the antenna [26].

$$x = R \sin \theta \quad (\text{A1})$$

and

$$y = R \cos \theta \quad (\text{A2})$$

where R is the distance from the antenna to the center point of the ellipse and θ is the incidence angle.

The major axis of the ellipse (a) is calculated by using the (A3).

$$a = a_1 + a_2 \quad (\text{A3})$$

where

$$a_1 = R \sin \left(\frac{\varphi_e}{2} \right) \sec \left(\theta + \frac{\varphi_e}{2} \right) \quad (\text{A4})$$

$$a_2 = R \sin \left(\frac{\varphi_e}{2} \right) \sec \left(\theta - \frac{\varphi_e}{2} \right) \quad (\text{A5})$$

where φ_e is the elevation angle.

The minor axis (b) is calculated by (A6).

$$b = 2R \tan \left(\frac{\varphi_{az}}{2} \right) \quad (\text{A6})$$

where φ_{az} is the azimuthal angle.

The area of Illumination (I) is equal to the area of ellipse and calculated by (A7).

$$I = \pi \left(\frac{a}{2} \right) \left(\frac{b}{2} \right) \quad (\text{A7})$$

Therefore,

$$I = \frac{\pi R^2}{2} \tan \left(\frac{\varphi_{az}}{2} \right) \sin \left(\frac{\varphi_e}{2} \right) \left[\sec \left(\theta + \frac{\varphi_e}{2} \right) + \sec \left(\theta - \frac{\varphi_e}{2} \right) \right] \quad (\text{A8})$$

The calculation of R is made by substituting the value of antenna parameter, i.e., φ_e , φ_{az} and θ and keeping the illumination area value 1 m^2 in (A8). Further, the calculation of x and y values, i.e., the position of antenna is made by substituting the values of R and θ in (A1) and (A2). It is assured that the beam must always illuminate the field of observation.

APPENDIX B. KIRCHHOFF SCALAR APPROXIMATION

Figure B1 represents the coordinate system for scattering geometry. (θ, φ) define the incident direction of the transmitted power $P_p(\theta, \varphi)$ at polarization p , and (θ_s, φ_s) is the direction of the received power $P_q(\theta_s, \varphi_s)$ at polarization q . Scattering coefficient under the scalar approximation is given by (B1) [27].

$$\sigma_{pq} = \sigma_{pqc} + \sigma_{pqn} + \sigma_{pqS} \quad (\text{B1})$$

where σ_{pqc} , σ_{pqn} and σ_{pqS} represent scattering coefficient due to coherent scattering, non-coherent scattering and scattering from surface slope, respectively.

$$\sigma_{pqc} = \pi k^2 |a_o|^2 \delta(q_x) \delta(q_y) e^{-q_z^2 s^2} \quad (\text{B2})$$

$$\sigma_{pqn} = (|a_o| k l / 2)^2 \exp(-q_z^2 s^2) \sum_n \left(\frac{(q_z^2 s^2)^n}{n! n} \right) \exp\left(-\frac{(q_x^2 + q_y^2) l^2}{4n}\right) \quad (\text{B3})$$

$$\begin{aligned} \sigma_{pqS} = & -(ksl)^2 (q_z/2) \exp(q_z^2 s^2) \operatorname{Re} \{a_o (q_x a_1^* + q_y a_2^*)\} \\ & \times \sum_{n=1}^{\infty} \left(\frac{(q_z^2 s^2)^{n-1}}{n! n} \right) \exp\left[-\frac{(q_x^2 + q_y^2) l^2}{4n}\right] \end{aligned} \quad (\text{B4})$$

Detailed expression regarding symbols in (B2), (B3) and (B4) can be found from the reference Ulaby et al. [26]. Here, $k=2\pi/\lambda$ where λ is

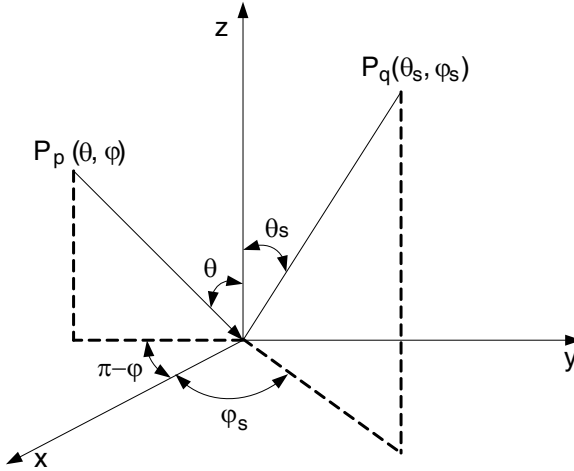


Figure B1. Coordinate system for scattering geometry.

wavelength. s and l are the rms surface height and correlation length respectively. $\delta(q_x)$ and $\delta(q_y)$ are Dirac delta functions. In case of specular scattering $\theta = \theta_s$, $\varphi = 0$ and $\varphi_s = 0$.

$$q_x = k (\sin \theta_s \cos \varphi_s - \sin \theta \cos \varphi) = 0 \quad (\text{B5})$$

$$q_y = k (\sin \theta_s \sin \varphi_s - \sin \theta \sin \varphi) = 0 \quad (\text{B6})$$

$$q_z = k (\cos \theta_s - \cos \theta) = 2k \cos \theta \quad (\text{B7})$$

Final expression of specular scattering coefficient for the Kirchhoff Scalar Approximation is given in (B8).

$$\sigma_{pqc} = \pi k^2 |a_o|^2 \delta(0) \delta(0) e^{-q_z^2 s^2} + (|a_o| k l/2)^2 \exp\left(- (2k \cos \theta)^2 s^2\right) \sum_n^{\infty} \left(\frac{\left((2k \cos \theta)^2 s^2 \right)^n}{n!n} \right) \quad (\text{B8})$$

Expression for a_o is polarization dependent. In case of HH -polarization a_o is give by (B9).

$$\begin{aligned} a_o &= -R_{\perp o} (\cos \theta + \cos \theta_s) \cos (\varphi_s - \varphi) \\ &= -R_{\perp o} (2 \cos \theta) = -2R_{\perp o} \cos \theta \end{aligned} \quad (\text{B9})$$

where $R_{\perp 0}$ is the Fresnel reflection coefficient for horizontal polarization and is given by (B10).

$$R_{\perp o} = \frac{\cos \theta - \sqrt{\varepsilon - \sin^2 \theta}}{\cos \theta + \sqrt{\varepsilon - \sin^2 \theta}} \quad (\text{B10})$$

In case of VV -polarization a_o is give by (B11).

$$\begin{aligned} a_o &= R_{\parallel o} (\cos \theta + \cos \theta_s) \cos (\varphi_s - \varphi) \\ &= R_{\parallel o} (2 \cos \theta) = 2R_{\parallel o} \cos \theta \end{aligned} \quad (\text{B11})$$

where $R_{\parallel 0}$ is the Fresnel reflection coefficient for vertical polarization and is given by (B12).

$$R_{\parallel o} = \frac{\varepsilon \cos \theta - \sqrt{\varepsilon - \sin^2 \theta}}{\varepsilon \cos \theta + \sqrt{\varepsilon - \sin^2 \theta}} \quad (\text{B12})$$

REFERENCES

1. Satalino, G., F. Mattia, M. W. J. Davidson, T. L. Toan, G. Pasquariello, and M. Borgeaud, "On current limits of soil moisture retrieval from ERS-SAR data," *IEEE Trans. Geosci. Remote Sens.*, Vol. 40, No. 11, 2438–2447, 2002.

2. Eangman, E. T. and N. Chauhan, "Status of microwave soil moisture measurements with remote sensing," *Remote Sens. Environ.*, Vol. 51, 189–198, 1995.
3. Brown, R. B., "Soil texture," University of Florida, IFAS Extension. Available: <http://edis.ifas.ufl.edu/SS169>, 2003.
4. Dubois, P. C., J. V. Zyl, and T. Engam, "Measuring soil moisture with imaging radars," *IEEE Trans. Geosci. Remote Sens.*, Vol. 33, No. 4, 915–926, 1995.
5. Davidson, M. W. J., F. Mattia, G. Satalino, N. E. C. Verhoest, T. L. Toan, M. Borgeaud, J. M. B. Louis, and E. Attema, "Joint statistical properties of RMS height and correlation length derived from multisite 1-m roughness measurements," *IEEE Trans. Geosci. Remote Sens.*, Vol. 41, No. 7, 1651–1658, 2003.
6. Paloscia, S., P. Pampaloni, S. Pettinato, and E. Santi, "A comparison of algorithms for retrieving soil moisture from ENVISAT/ASAR images," *IEEE Trans. Geosci. Remote Sens.*, Vol. 46, No. 10, 3274–3284, 2008.
7. Singh, D., "A simplistic incidence angle approach to retrieve the soil moisture and surface roughness at X-Band," *IEEE Trans. Geosci. Remote Sens.*, Vol. 43, No. 11, 2606–2611, 2005.
8. Singh, D. and A. Kathpalia, "An efficient modeling with GA approach to retrieve soil texture, moisture and roughness from ERS-2 SAR data," *Progress In Electromagnetics Research*, Vol. 77, 121–136, 2007.
9. Mittal, G. and D. Singh, "Critical analysis of microwave scattering response on roughness parameter and moisture content for periodic rough surfaces and its retrieval," *Progress In Electromagnetics Research*, Vol. 100, 129–152, 2010.
10. Singh, D. and V. Dubey, "Microwave bistatic polarization measurements for retrieval of soil moisture using an incidence angle approach," *J. Geophys. Eng.*, Vol. 4, 75–82, 2007.
11. Ceraldi, E., G. Franceschetti, A. Iodice, and D. Riccio, "Estimating the soil dielectric constant via scattering measurements along the specular direction," *IEEE Trans. Geosci. Remote Sens.*, Vol. 43, No. 2, 295–305, 2005.
12. De Roo, R. D. and F. T. Ulaby, "Bistatic specular scattering from rough dielectric surfaces," *IEEE Trans. Antennas Propag.*, Vol. 42, No. 2, 220–231, 1994.
13. Nashashibi, A. Y., and F. T. Ulaby, "MMW polarimetric radar bistatic scattering from a random surface," *IEEE Trans. Geosci. Remote Sens.*, Vol. 45, No. 6, 1743–1755, 2007.

14. Prakash, R., D. Singh, and N. P. Pathak, "Microwave specular scattering response of soil texture at X-band," *Advances in Space Research*, Vol. 44, 801–814, 2009.
15. Pierdicca, N., L. Pulvirenti, F. Ticconi, and M. Brogioni, "Radar bistatic configuration for soil moisture retrieval: A simulation study," *IEEE Trans. Geosci. Remote Sens.*, Vol. 46, No. 10, 3252–3264, 2008.
16. Wu, T., K. Chen, J. Shi, H. Lee, and A. K. Fung, "A study of an AIEM model for bistatic scattering from randomly rough surface," *IEEE Trans. Geosci. Remote Sens.*, Vol. 46, No. 9, 2584–2598, 2008.
17. Krieger, G., H. Fiedler, D. Hounam, and A. Moreira, "Analysis of system concepts for bi- and multi-static SAR missions," *IEEE Geoscience and Remote Sensing Symposium Proceedings*, 770–772, Toulouse, France, Jul. 21–25, 2003.
18. Du, Y., Y. Qi, H. Chen, and J. A. Kong, "Bistatic scattering model for rough surfaces," *IEEE Geoscience and Remote Sensing Symposium Proceedings*, 2949–2952, Denver, USA, Jul. 31–Aug. 4, 2006.
19. Comblet, F., A. Khenchaf, A. Baussard, and F. Pellen, "Bistatic synthetic aperture radar imaging: Theory, simulations, and validations," *IEEE Trans. Geosci. Remote Sens.*, Vol. 54, No. 11, 3529–3540, 2006.
20. TanDEM-X—a valuable partner for TerraSAR-X Available: <http://www.infoterra.de/terrasar-x/tandem-x-mission.html>.
21. Mironov, V. L., M. C. Dobson, V. H. Kaupp, S. A. Komarov, and V. N. Kleshchenko, "Generalized refractive mixing dielectric model for moist soils," *IEEE Trans. Geosci. Remote Sens.*, Vol. 42, No. 4, 773–785, 2004.
22. Hallikainen, M. T., F. T. Ulaby, M. C. Dobson, M. A. El-Rayes, and L. Wu, "Microwave dielectric behavior of wet soil-part I: Empirical models and experimental observations," *IEEE Trans. Geosci. Remote Sens.*, Vol. 23, No. 1, 25–34, 1985.
23. Wang, J. R., and T. J. Schmugge, "An empirical model for the complex dielectric permittivity of soil as a function of water content," *IEEE Trans. Geosci. Remote Sens.*, Vol. 18, No. 4, 288–295, 1980.
24. Boyarskii, D. A., V. V. Tikhonov, and N. Y. Komarova, "Model of dielectric constant of bound water in soil for applications of microwave remote sensing," *Progress In Electromagnetics Research*, Vol. 35, 251–269, 2002.

25. Apparao, K. V. S. and V. C. S. Rao, *Soil Testing-laboratory Manual and Question Bank*, 18–28, Laxmi Publication, New Delhi, 1995.
26. Trebits, R. N., “Radar cross section,” *Radar Reflectivity Measurement: Technique and Applications*, N. C. Curie, Ed., 51–59, Artech House, Norwood, MA, 1989.
27. Ulaby, F. T., R. K. Moore, and A. K. Fung, *Microwave Remote Sensing — Active and Passive*, Vol. 2, 921–949, Artech House, Norwood, MA, 1982.